Published in final edited form as:
Exp Eye Res. 2010 January ; 90(1): 10–16. doi:10.1016/j.exer.2009.09.001.

Estrogen Receptor β protects against *in vivo* injury in RPE cells

Sharon J. Elliot, Ph.D.[1,*], **Paola Catanuto**[1], **Diego G. Espinosa-Heidmann, M.D.**[2], **Pedro Fernandez**[1], **Eleut Hernandez**, **Peter Saloupis**[4], **Kenneth Korach, Ph.D.**, **Michael Karl**[1], and **Scott W. Cousins, M.D**[4]

[1] Laboratory on Sex and Gender Differences in Health and Disease, University of Miami, Miller School of Medicine, Miami, Florida

[2] Department of Ophthalmology, Medical College of Georgia, Augusta, Georgia

[3] Receptor Biology Laboratory, National Institutes of Environmental Health Science, Research Triangle Park

[4] Duke Center for Macula Diseases, Duke University Eye Center, Durham, NC

Abstract

Epidemiological data suggest that estrogen deficiency in post menopausal women may contribute to the severity of AMD. We discovered that 17β-estradiol (E_2) was a crucial regulator of the severity of extracelllular matrix turnover (ECM) dysregulation both in vivo and in vitro. We also found in vitro that the presence of estrogen receptor (ER)β regulates MMP-2 activity. Therefore in an attempt to delineate the role of the ER subtypes, female estrogen receptor knockout (ERKO) mice were fed a high-fat diet, and the eyes were exposed to seven 5-second doses of nonphototoxic levels of blue-green light over 2 weeks. Three months after cessation of blue light treatment, transmission electron microscopy was performed to assess severity of deposits, Bruchs membrane changes, and choriocapillaris endothelial morphology. We found that changes in the trimolecular complex of proMMP-2, MMP-14 and TIMP-2 correlated with increased Bruch's membrane thickening or sub retinal deposit formation (basal laminar deposits) in ERKOβ mice. In addition RPE isolated from ERKO β mice had an increase in expression of total collagen and a decrease in MMP-2 activity. Finally we found that ERK an intermediate signaling molecule in the MMP pathway was activated in RPE isolated from ERKOβ mice. These data suggest that mice which lack ERβ are more susceptible to in vivo injury associated with environmental light and high fat diet.

Introduction

Epidemiologic data suggest that estrogen is protective against age related macular degeneration (AMD), but that severity of AMD in women (as compared to men) increases in proportion to duration from onset of menopause (2009). In that regard, controversy exists regarding the use of estrogens or other hormone replacement therapy (HRT) and its relationship to AMD (Cumming and Mitchell, 1997;Freeman et al., 2005;Haan et al., 2006). Recently, the Women's Health Initiative Sight Exam study on hormone therapy and AMD revealed that treatment with conjugated equine estrogens and progesterone did not influence the occurrence of early AMD although it may reduce the risk of soft drusen or wet AMD. Another large study found a reduced

*Corresponding Author: Sharon Elliot, Ph.D., Miller School of Medicine, University of Miami, Rosenstiel Medical Building Room 1043, R104, Miami, Fl, 33136.

risk of large drusen, but not AMD. Several other studies suggest that there is a reduced risk of AMD with postmenopausal hormone replacement therapy (HRT). Differences between these studies may be due to timing of initiation and type of HRT and were unfortunately not addressed.

Estrogens (E_2) physiologic effects are mediated by two estrogen receptor subtypes, ERα and ERβ (Bjornstrom and Sjoberg, 2005;McDonnell, 2004) These ER subtypes exhibit both differential and overlapping expression in various tissues (Couse et al., 1997). We and others have previously shown that both subtypes are present and active in retinal pigmented epithelial (RPE) cells isolated from human male and female eyes (Marin-Castano et al., 2003;Ogueta et al., 1999). In addition, we reported that E_2 deficiency in female middle aged C57Bl/6 mice leads to increased Bruch's membrane thickening with sub-RPE deposit formation (Cousins et al., 2003) and that aging females have worse deposits than aged males in models of both dry and wet AMD (Cousins et al., 2003;Espinosa-Heidmann et al., 2005).

We previously found that E_2 regulates normal extracellular matrix (ECM) turnover of human and mouse RPE cells at least in part by regulation of MMP-2 activity (Elliot et al., 2008;Marin-Castano et al., 2003). We also found that the components of the trimolecular complex, matrix metalloproteinase (MMP)-2, MMP-14 and tissue inhibitor of metalloproteinase (TIMP)-2 activity are regulated *in vitro* in an estrogen receptor (ER) subtype specific (Elliot et al., 2008). We therefore hypothesized that changes in MMP-2 regulation may lead to early dry AMD and that estrogens could play a role in preventing these changes. In this study we investigated whether genetically altered mice that lack either ERα or ERβ may be more susceptible to *in vivo* injury associated with environmental light and high fat diet. We also determined whether extracellular signal-regulated kinases (ERK) activation, a potential intermediate signaling molecule in the regulation of MMP-2 activity, was preferentially regulated by ER subtypes in the RPE.

Methods

Mice

Female estrogen receptor knockout (ERKO) mice on a C57Bl/6 background were obtained from the National Institute of Environmental Health Sciences, National Institutes of Health. The guidelines of the ARVO Statement for the Use and Care of Animals in Ophthalmic and Vision Research were followed, and the Division of Veterinary Resources approved all experiments.

Experimental Model for Sub-RPE Deposits

As previously described experimental mice were switched from a regular diet (Diet 5001; PMI Nutrition International Test Diet, Richmond, IN) to high-fat chow (Diet 5015; PMI Nutrition International Test Diet) at 10 months of age, to allow tissue distribution of lipid from the diet. The high-fat diet more than doubled the relative percentage of calories from fat but maintained the same number of calories per gram of food (by reducing the percentage of calories from carbohydrates) (Cousins et al., 2002). At approximately 11 months of age, a repetitive exposure to nonphototoxic levels of argon laser 488 nm blue-green light (Model 910A Argon Laser; Coherent, Palo Alto, CA) was used to induce transient production of RPE oxidant (Cousins et al., 2002). Briefly, the eyes were dilated, the mice anesthetized, and exposed to seven 5-second exposures to 20 mJ (approximately one third the threshold intensity to produce a clinical lesion) of argon laser 488-nm blue-green light. This was administered 2 to 3 days apart over a 2-week period (Cousins et al., 2002). The high-fat diet was continued for three additional months, after the 2-week exposure to blue-green light. Mice were then sacrificed at 15 months of age and

the eyes immediately removed for transmission electron microscopy (TEM), and isolation of RPE cells for MMP-2 zymography and Western blot analysis.

RPE Isolation

After enucleation, the eyes were rinsed with 10% gentamicin for sterilization and twice with PBS (1×). The eyes were then placed in a dish containing PBS (1×) and with the aid of a dissecting microscope, were opened by a circumferential incision at the ora serrata. The anterior segment was removed, and the vitreous-retina was separated from the RPE and choroid eyecup with a round-tipped disposable blade (K20-1504; Katena Products, Inc., Denville, NJ) and Tennant forceps (K5-5230; Katena Products, Inc.). The remaining eyecup was incubated with Dulbecco's modified Eagle's medium (DMEM)/F12 (1:1 vol/vol) supplemented with 10% fetal bovine serum (FBS) at 37°C for 10 minutes. Then, using a Barraquer spatula (K3-2310; Katena Products, Inc.) for blunt dissection and scraping, the RPE monolayer was dissected from BrM and choroid. The RPE from the right and the left eye was aspirated with a micropipette and either stored at −80°C until protein extraction and analysis or plated as described for propagation of cell lines (Elliot et al., 2008).

An aliquot from the isolated RPE cells were stained with mouse anti-cytokeratin-18 antibody (Sigma, St. Louis, MO) and with mouse anti-endothelial cell (CD146) monoclonal antibody (Chemicon International, Inc., Temecula, CA) to ensure that there was no contamination with endothelial cells. All experiments were performed on cells between passages 4–8.

Histology and TEM

Mice were killed by anesthetic overdose and perfused with saline followed by a mixture of 3% glutaraldehyde and 2% paraformaldehyde. Eyes were immediately enucleated and the corneas removed and fixed in 3% glutaraldehyde and 2% paraformaldehyde in PBS (0.1 M, pH 7.3) overnight. The lens was removed, and the posterior segment (retina, choroid, and sclera) was quadrisected to contain the perioptic nerve portion at the apex and the ciliary body at the base. The superotemporal quadrant of retina, choroid, and sclera was submitted for electron microscopic sectioning. The tissue was fixed in 1% osmium tetroxide for 1 hour, rinsed in PBS, dehydrated in EtOH, and then imbedded in Spur's resin. Thick and ultrathin sections (0.7–1.0 μm) were cut on a microtome (MT-2; Porter Blum, Hatfield, PA). Thick sections were stained with toluidine blue and examined by light microscopy. Ultrathin sections were stained with 4% uranyl acetate and lead citrate and examined with a transmission electron microscope (model CX-100; JEOL, Tokyo, Japan).

Semiquantitative Grading System

For each specimen, a single cross-section was examined, and low-power transmission electron micrographs were made of the entire section from perioptic to ciliary body portion (approximately 10 micrographs). Then, two to four representative high-power micrographs were made from each low-power section, by an individual unaware of the experimental conditions, and were used for semiquantitative scoring. The low- and high-power micrographs were graded by two independent examiners for the presence and severity of BLD. Low-power micrographs were useful for orientation, quality of the sectioning (i.e. the external outer segment disc of the photoreceptors helped to account for obliqueness of the sectioning), and extension of the sub-RPE deposits. High-power micrographs were used for the more detailed analysis of our classification. A severity score of 0 to 15 points was determined for each section by summation of the median scores of all the micrographs from a section on each of five different categories of abnormalities (from 0 to 3 points for each): 1. continuity of basal laminar deposits (BLD); 2. maximal thickness of BLD; 3. nature of deposit content (homogeneous, banded structures, membranous debris, granular material); 4. presence of bruch's membrane (BrM) abnormalities (including thickness analysis); and 5. assessment of other choriocapillaris

endothelial damage or invasion. BrM thickness was also directly measured in three different standardized locations in each image and then averaged to provide a mean score for that micrograph. The mean of 12 high-power micrographs was used to assign and average BrM thickness for an individual specimen.

Groups were compared by determining the mean ± SD, and the *t*-test was used for statistical analysis of the differences. In addition, the frequency of BLD was determined using two different criteria. “Any BLD” was defined as the presence of any discrete focal nodule of homogenous material of intermediate electron density between the RPE cell membrane and BrM in at least one micrograph within a section. “Moderate BLD” was defined as the presence, in at least three micrographs, of the following: continuous BLD extending under two or more cells, deposit thickness equal to or greater than 20% of RPE cell cross-sectional thickness, or the presence of any banded structures within the BLD. Differences in the relative frequency were tested using ^{2} analysis (Cousins et al., 2002).

Cell Culture

RPE cells were isolated and propagated as previously described. Briefly, intact sheets of RPE cells were collected and centrifuged. Cells were suspended in Dulbecco’s modified medium (DMEM) and 10% fetal bovine serum and added to the upper chamber of a transwell insert. After an initial growth period, the cells were trypsinized and grown in larger flasks to prepare for immortalization (Catanuto et al., 2009). Cells were allowed to come to confluence for 7–10 days before experiments were initiated since these cell lines were transformed and can detach from the dish after an extended period of time. We have shown however, that they retain many of their in vivo characteristics (Catanuto et al., 2009;Elliot et al., 2008). All experiments were performed in estrogen-free DMEM medium and charcoal stripped serum to prevent stimulation of the estrogen receptor.

Microarray analysis

Total RNA was prepared as previously described (Elliot et al., 2008). The quality of the RNA sample was analyzed on a Agilent 2100 Bioanalyzer. Briefly, approximately 100 to 200 ng of the sample was placed in an RNA LabChip with the appropriate sample loading buffer and electrophoresed in parallel with an RNA standard ladder (Ambion/Applied Biosystems, Austin Tx). Agilent Technologies’ Bioanalyzer software was used to analyze the results and to create an electropherogram. RNA was considered usable if ratio of 28S ribosomal peak to 18 S ribosomal peak was above 1.0.

Labeling and Hybridization

10μg of total RNA was amplified and labeled using Amino Allyl MessageAmp aRNA Amplification Kit (Ambion/Applied Biosystems, Austin Tx) and Cy3- and Cy5-NHS ethers (Amersham, Piscataway, NJ). Concentration of the labeled aRNA and labeling efficiency were determined spectrophotometrically, and equal amounts of labeled aRNA were hybridized to Agilent Whole Mouse Genome Oligo microarrays for 17 hours at 65°C according to manufacturer’s instructions.

Image Analysis and Data Processing

The microarrays were scanned at a 10 micron resolution using a GenePix 4000A scanner (Molecular Devices) and the resulting images were analyzed with the software package GenePix Pro 5.1 (Molecular Devices). Data extracted from the images were transferred to the software package Acuity 4.0 (Molecular Devices) for normalization and statistical analysis. Each array was normalized for signal intensities across the whole array and locally, using Lowess normalization. Features for further analysis were selected according to the following

quality criteria: 1) at least 90% of the pixels in the spot had intensity higher than background plus two standard deviations; 2), there were less than 2% saturated pixels in the spot; 3) signal to noise ratio (defined as ratio of the background subtracted mean pixel intensity to standard deviation of background) was 3 or above for each channel; 4) the spot diameter was between 80 and 110 micron; 5) the regression coefficient of ratios of pixel intensity was 0.6 or above.

To identify significantly expressed genes across all replicate arrays one-class SAM (Significant Analysis of Microarray, http://www-stat.stanford.edu/~tibs/SAM) (Tusher et al., 2001) analysis was used with the smallest FDR (False Discovery Rate). All primary microarray data were submitted to the public database at the GEO web site (http://www.ncbi.nih.gov/geo). Selected genes were classified according to Gene Ontology category "biological process" using Onto-Express (http://vortex.cs.wayne.edu/Projects.html) (Draghici et al., 2003;Khatri et al., 2002).

Real time RT-PCR

Real RT-PCR was performed as previously described (Elliot et al., 2006). Briefly, real-time RT-PCR reactions were performed using the TaqMan One Step RT-PCR Master mix reagent kit and the ABI step one real time machine in a total volume of 25ul of reaction mixture. Data are expressed as the ratio of the target molecule to 18s.

Collagen Assay

Total soluble collagen production was measured in the supernatants of RPE cells using the Sircol Assay (Biodye Science, UK) according to manufacture's directions. Briefly, cell supernatants were collected from RPE cell monolayers and treated with syrius red dye which binds to the [Gly-X-Y] tripeptide end sequence of mammalian collagen. The solubilized collagen was measured by an optical density analysis at 595 nm. The amount of collagen was calculated based on a standard curve.

MMP-2 Activity

RPE cell supernatants were collected, and cell number determined as previously described (Elliot et al., 2006). MMP-2 activity was assessed with 10% zymogram gels (Invitrogen Corp., Carlsbad, CA), as described previously. Briefly, the medium was diluted to normalize for cell number before the addition of 5× Laemmli buffer under nonreducing conditions. After electrophoresis, gels were washed for 1 hour in 2.5% Triton X-100 and incubated 24 hours in 50 mM Tris buffer. The gels were stained with Coomassie Blue and air dried. Densitometry, using NIH image version 1.6 (available by ftp from zippy.nimh.nih.gov/or from http://rsb.info.nih.gov/nih-image developed by Wayne Rasband, National Institutes of Health, Bethesda, MD) was used to analyze relative MMP-2 activity. Each zymography assay was repeated at least three times.

Western analysis

Protein lysates were electrophoresed and probed with an antibody to either total ERK1/2 or the corresponding phophorylated forms (Santa Cruz Biotechnology Inc, Santa Cruz, CA) as previously described (Karl et al., 2005).

Statistics

Data from real time PCR experiments are expressed as the ratio of ERKO to wildtype. Data from statistical analysis of zymography, and Western blot analysis are expressed as percentage of control (wild type littermate). One-way analysis of variance and the Dunnett multiple-comparison post hoc test or Student's *t*-test were performed for the statistical analysis.

Results

There was no difference in body weight between ERα littermate controls and αERKO mice (43.2 ± 3.3 vs 47.9 ± 3.7) or βERKO vs αERKO mice (58.6 ±1.8 vs 47.9 ± 3.7). However, there was an increase in body weight between ERβ littermate controls and βERKO mice (43.7 ±3.9 vs 58.9±1.8, $p<0.05$).

TEM

TEM revealed the presence of sub-retinal deposit formation which was found to be more severe in eyes isolated from ERKOβ mice (Figure 1B, severity score 5–7) compared to either ERKOα (Figure 1A, score 1–2) or littermate controls (Figure 1C, 0–2) or normal aging (<1) (Table 1A and 1B). ERKOβ mice micrographs showed extensive amorphous accumulation of material with intermediate electron density between the RPE cell membrane and its basal membrane. This material has been identified as basal laminar deposits (BLD) often containing additional structures especially fibrous long spaced collagen represented by banded structures. Destruction of membranous folds can be appreciated in these ERKOβ mice as opposed to littermate controls or ERKOα mice. There was also evidence of a significant thickening of Bruch's membrane in ERKβO mice as opposed to the other groups.

Cell culture

In order to study RPE, cell lines were isolated from ERKO mice and littermate controls as described (Catanuto et al., 2009;Elliot et al., 2008). RPE cells expressed RPE65 mRNA and protein and CRALPB protein. There was no apparent difference in morphology. The variation in growth between cell lines was not related to the presence or absence of ERβ.

Microarray data

Microarray analysis was performed on littermate control and ERKO RPE cell lines. Collagen type I (α1 and α2 chains) and type III (α1) were increased almost 3 fold in ERKO β cells compared to ERKOα cell lines. Collagen type 1 and type VI, tenascin and fibronectin were also increased at least 2 fold compared to littermate control cells.

Realtime PCR

We confirmed by real-time RT-PCR the more than 2 fold increase mRNA expression of collagen type I in ERKOβ RPE cell lines compared to wt littermates as well as ERKOα cell lines. mRNA expression of MMP-2 (*$p<0.05$) and MMP-14 ($p=0.05$) were decreased at least 2–3 fold compared to ERKOα cell lines (Figure 2). In contrast, TIMP-2 expression was not different between any of the groups.

MMP-2 activity

MMP-2 activation requires a tri-molecular complex between pro-MMP-2, MMP-14, and TIMP-2. Since there appeared to be a change in ratio between the mRNA expression of the components of the tri-molecular complex, we assessed MMP-2 activity levels by zymography. Both pro and active MMP-2 were significantly decreased In ERKOβ cells (Figure 3) compared to littermate controls and ERKOα cell lines, ($p<0.05$). These data were in agreement with the mRNA expression data.

Collagen Assay

MMPs are crucial regulators of basement membrane and ECM turnover. Accordingly, loss of RPE MMP activity most likely leads to excessive accumulation of collagen. We found that total collagen production increased in cells isolated from ERKOβ mice compared to those of ERKOα mice (Figure 4, *$p<0.05$).

Western analysis of ERK

Multiple studies have shown that MMP-2 activity is regulated through the MAPK signaling pathway although the contribution of estrogen receptors to that cascade has not been explored. The phosphorylation of ERK was dependent on the presence or absence of ERβ (Figure 5). Both ERK 1 and ERK 2 were activated in the absence of ERβ compared to littermate control and ERKOα cell lines. Interestingly total ERK was also regulated based on the presence or absence of ERβ (Figure 5).

Discussion

In this study we evaluated the role of ERβ in the regulation of severity of sub-retinal deposit formation and RPE ECM expression in mice. We fed ERKOα, ERKOβ and littermate control mice a high fat diet and treated them with blue light as previously described (Cousins et al., 2002). Knockout of ERβ was associated with more severe Bruch's membrane (BrM) thickening, and accumulation of sub-retinal deposits (i.e., BLD) which were not present in littermate controls or were less severe in ERKOα mice. These studies expand our previous findings that estrogen plays an important role in the maintenance of normal ECM turnover and address the question of the role of ER subtypes in this preservation.

AMD, a disease of the elderly, is twice as prevalent in aging postmenopausal women compared to same-age men. Although this may be attributed to the longevity of women as compared to men (Adminstration on Aging, 2005), studies of estrogen or combined estrogen/progestin replacement therapy have delivered equivocal results in regard to its effects on the development and progression of AMD in elderly women (Cumming and Mitchell, 1997;Freeman et al., 2005;Haan et al., 2006). In contrast, the data obtained by several, albeit smaller studies, suggested that HRT reduced the risk of AMD in postmenopausal woman. Timing of the initiation and the different types of sex hormones used for replacement therapy were not addressed in these studies which could account for their different study outcomes.

We have previously shown that a relatively small dysregulation in the ratio of MMPs and collagens can produce profound changes in the ECM, including thickening of BrM and deposit formation (Elliot et al., 2006;Marin-Castano et al., 2005;Marin-Castano et al., 2006). In this study we show that the absence of ERβ *in vivo* leads to baseline changes in the mRNA expression of the components of the trimolecular complex and subsequent decreased MMP-2 activity. In addition, we found an increase in total collagen production as well as collagen type I mRNA expression and other BrM components. These data suggest that the decrease in MMP-2 activity correlates to an increase in collagen deposition and potentially sub-retinal deposit formation. Although the effects of estrogens on MMP-2 activation as well as collagen gene regulation are well known in smooth muscle cells (Wingrove et al., 1998), glomerular cells (Karl et al., 2006) and RPE cells (Elliot et al., 2008), to our knowledge this is the first time that MMP-2 activity changes and ECM dysregulation in the retina is documented *in vivo* using ERKO mice. Importantly, RPE cells lacking ERβ had decreased MMP-14 activity after *in vivo* injury similar to our findings *in vitro* (Elliot et al., 2008). MMP-14 not only plays a role in activation of MMP-2 but directly degrades collagens, suggesting an additional mechanism for the increase in collagens types I and III. Interestingly RPE cells without ERα had a higher expression of MMP-14 than their littermate controls which may also afford some protection against the oxidant induced injury.

Estrogen receptors mediate many of the biological actions of estrogens although tissue and cell distribution of ER subtypes varies. Our group and several others have reported the presence of both ER subtypes in the human, bovine and rat retina (Kobayashi et al., 1998;Munaut et al., 2001;Ogueta et al., 1999) and human and mouse RPE cells (Catanuto et al., 2009;Elliot et al., 2003;Marin-Castano et al., 2003). Following ligand binding, ERs form dimers. The presence

of both subtypes in RPE cells suggest the potential to form ERα/ERβ heterodimers, which would predict complex patterns of gene expression not observed by either homodimer alone. Although the function and/or action of ERα has been described in greater detail than ERβ, recent studies using ERβ null (ERKOβ) mice or ERβ selective agonists have indicated that ER β plays a role in inflammation, the immune system (Cvoro et al., 2008) and prostate health and disease (Prins and Korach, 2008).

Our results led us to speculate on the possible interactions of ERα and ERβ in intact RPE cells. Our published study on isolated RPE cells that were exposed to oxidant injury *in vitro*, showed that in the presence of the natural ligand E_2, ERβ/Sp1 interactions are necessary for regulation of the MMP-2 promoter activity (Elliot et al., 2008). Similarly, in some tissues the ERα/Sp1 interaction induces transcription while the formation of ERβ/Sp1 does not (Saville et al., 2000). It is tempting to think that environmental injury induces changes in the ER subtype ratio which make the RPE more vulnerable and lead to subsequent dysregulation of ECM turnover. In osteoblasts for example, collagen type 1 production changes in response to alterations in ERα/ERβ ratios (Monroe et al., 2005). In addition, changes in subtype ratio have also been documented in aging. Future studies in our laboratory will address these important changes in our injury model.

Finally we assessed the ERK signaling pathway which coordinates cellular responses to oxidative stress and regulates MMP-2 activity. Since estrogens have also been shown to regulate ERK via ER-dependent and independent mechanisms (Levin, 2003), we postulated that either directly or through crosstalk, ERK activation might be regulated by the presence or absence of ERβ. Relevant to our study, a series of recent investigations using Lewis lung carcinoma cell lines and human cervical cancer cells showed that induction of the ERK and PI3K pathways have a regulatory effect on synthesis of both MMP-2 and MMP-14 without an effect on TIMP-2 synthesis (Kharas and Fruman, 2005;Zhang and Brodt, 2003). In a recent study by Nagai et al (Nagai et al., 2008) ERK activation was an intermediate signaling event in the CTGF induction of matrix production in ARPE-19 cells. Indeed we found that in cell lines isolated from mice without ERβ, ERK activation increased at least 2 fold compared to cells isolated from either littermate controls or ERKOα mice.

In summary C57Bl6 mice that lack ERβ are more susceptible to injury induced by environmental light and high fat diet. The lack of ERβ leads to more severe sub-retinal deposit formation with BLD compared to littermate controls and mice that lack ERα. In addition, the trimolecular components that regulate MMP-2 activation are altered leading to a decrease in MMP-2 activity and increased collagen production. ERK activation in RPE cells isolated from ERKOβ mice could lead to changes in ECM turnover through regulation of MMPs. These data suggest that targeting ERβ may have important therapeutic implications for treatment of early AMD.

Acknowledgments

This work was supported in part by National Institutes of Health, National Eye Institute Grant RO1 EY1447-04 (SJE, MK, and SWC)

Grants: this work was supported in part by National Institutes of Health National Eye Institute Grant RO1 EY14477-04 (SJE and SWC).

Reference List

Age-Related Macular Degeneration. National Eye Institute; 2009.

Adminstration on Aging. Older Women. 2005. www.aoa.gov

Bjornstrom L, Sjoberg M. Mechanisms of estrogen receptor signaling: convergence of genomic and nongenomic actions on target genes. Mol Endocrinol 2005;19:833–42. [PubMed: 15695368]

Catanuto P, Espinosa-Heidmann D, Pereira-Simon S, Sanchez P, Salas P, Hernandez EP, Cousins SW, Elliot SJ. Mouse Retinal Pigmented Epithelial Cell Lines retain their phenotypic characteristics after transfection with Human Papilloma Virus: A new tool to further the study of RPE biology. Exp Eye Res 2009;88:99–105. [PubMed: 19013153]

Couse JF, Lindzey J, Grandien K, Gustafsson JA, Korach KS. Tissue distribution and quantitative analysis of estrogen receptor-α (ERα) and estrogen receptor-β (ERβ) messenger ribonucleic acid in the wild-type and ERα-knockout mouse. Endocrinology 1997;138:4613–21. [PubMed: 9348186]

Cousins SW, Espinosa-Heidmann DG, Alexandridou A, Sall J, Dubovy S, Csaky K. The role of aging, high fat diet and blue light exposure in an experimental mouse model for basal laminar deposit formation. Exp Eye Res 2002;75:543–53. [PubMed: 12457866]

Cousins SW, Marin-Castano ME, Espinosa-Heidmann DG, Alexandridou A, Striker L, Elliot S. Female gender, estrogen loss, and Sub-RPE deposit formation in aged mice. Invest Ophthalmol Vis Sci 2003;44:1221–9. [PubMed: 12601052]

Cumming RG, Mitchell P. Hormone Replacement Therapy, Reproductive Factors, and Cataract The Blue Mountains Eye Study. Am J Epidemiol 1997;145:242–9. [PubMed: 9012597]

Cvoro A, Tatomer D, Tee MK, Zogovic T, Harris HA, Leitman DC. Selective Estrogen Receptor-Agonists Repress Transcription of Proinflammatory Genes. J Immunol 2008;180:630–6. [PubMed: 18097065]

Draghici S, Khatri P, Martins RP, Ostermeier GC, Krawetz SA. Global functional profiling of gene expression. Genomics 2003;81:98–104. [PubMed: 12620386]

Elliot S, Catanuto P, Fernandez P, Espinosa-Heidmann D, Karl M, Korach K, Cousins SW. Subtype Specific Estrogen Receptor Action Protects Against changes in MMP-2 Activation in Mouse Retinal Pigmented Epithelial Cells. Exp Eye Res 2008;86:653–60. [PubMed: 18313050]

Elliot S, Catanuto P, Stetler-Stevenson W, Cousins SW. Retinal Pigment Epithelium Protection From Oxidant-mediated Loss of MMP-2 Activation Requires Both MMP-14 and TIMP-2. Invest Ophthalmol Vis Sci 2006;47:1696–702. [PubMed: 16565411]

Elliot SJ, Karl M, Berho M, Potier M, Zheng F, Leclercq B, Striker GE, Striker LJ. Estrogen deficiency accelerates progression of glomerulosclerosis in susceptible mice. Am J Pathol 2003;162:1441–8. [PubMed: 12707027]

Espinosa-Heidmann DG, Marin-Castano ME, Pereira-Simon S, Hernandez EP, Elliot S, Cousins SW. Gender and estrogen supplementation increases severity of experimental choroidal neovascularization. Exp Eye Res 2005;80:413–23. [PubMed: 15721623]

Freeman EE, Munoz B, Bressler SB, West SK. Hormone replacement therapy, reproductive factors, and age-related macular degeneration: the Salisbury Eye Evaluation Project. Ophthalmic Epidemiol 2005;12:37–45. [PubMed: 15848919]

Haan MN, Klein R, Klein BE, Deng Y, Blythe LK, Seddon JM, Musch DC, Kuller LH, Hyman LG, Wallace RB. Hormone Therapy and Age-Related Macular Degeneration: The Women's Health Initiative Sight Exam Study. Arch Ophthalmol 2006;124:988–92. [PubMed: 16832022]

Karl M, Berho M, Pignac-Kobinger J, Striker GE, Elliot SJ. Differential effects of continuous and intermittent 17beta-estradiol replacement and tamoxifen therapy on the prevention of glomerulosclerosis: modulation of the mesangial cell phenotype in vivo. Am J Pathol 2006;169:351–61. [PubMed: 16877338]

Karl M, Potier M, Schulman IH, Rivera A, Werner H, Fornoni A, Elliot SJ. Autocrine activation of the local insulin-like growth factor I system is up-regulated by estrogen receptor (ER)-independent estrogen actions and accounts for decreased ER expression in type 2 diabetic mesangial cells. Endocrinology 2005;146:889–900. [PubMed: 15550505]

Kharas MG, Fruman DA. ABL oncogenes and phosphoinositide 3-kinase: mechanism of activation and downstream effectors. Cancer Res 2005;65:2047–53. [PubMed: 15781610]

Khatri P, Draghici S, Ostermeier GC, Krawetz SA. Profiling gene expression using onto-express. Genomics 2002;79:266–70. [PubMed: 11829497]

Kobayashi K, Kobayashi H, Ueda M, Honda Y. Estrogen receptor expression in bovine and rat retinas. Invest Ophthalmol Vis Sci 1998;39:2105–10. [PubMed: 9761289]

Levin ER. Bidirectional signaling between the estrogen receptor and the epidermal growth factor receptor. Mol Endocrinol 2003;17:309–17. [PubMed: 12554774]

Marin-Castano ME, Csaky KG, Cousins SW. Nonlethal oxidant injury to human retinal pigment epithelium cells causes cell membrane blebbing but decreased MMP-2 activity. Invest Ophthalmol Vis Sci 2005;46:3331–40. [PubMed: 16123437]

Marin-Castano ME, Elliot SJ, Potier M, Karl M, Striker LJ, Striker GE, Csaky KG, Cousins SW. Regulation of estrogen receptors and MMP-2 expression by estrogens in human retinal pigment epithelium. Invest Ophthalmol Vis Sci 2003;44:50–9. [PubMed: 12506055]

Marin-Castano ME, Striker GE, Alcazar O, Catanuto P, Espinosa-Heidmann DG, Cousins SW. Repetitive nonlethal oxidant injury to retinal pigment epithelium decreased extracellular matrix turnover in vitro and induced sub-RPE deposits in vivo. Invest Ophthalmol Vis Sci 2006;47:4098–112. [PubMed: 16936130]

McDonnell DP. The molecular determinants of estrogen receptor pharmacology. Maturitas 2004;48 (Suppl 1):S7–12. [PubMed: 15337242]

Monroe DG, Secreto FJ, Subramaniam M, Getz BJ, Khosla S, Spelsberg TC. Estrogen receptor alpha and beta heterodimers exert unique effects on estrogen- and tamoxifen-dependent gene expression in human U2OS osteosarcoma cells. Mol Endocrinol 2005;19:1555–68. [PubMed: 15802376]

Munaut C, Lambert V, Noel A, Frankenne F, Deprez M, Foidart JM, Rakic JM. Presence of oestrogen receptor type {beta} in human retina. Br J Ophthalmol 2001;85:877–82. [PubMed: 11423466]

Nagai N, Klimava A, Lee WH, Izumi-Nagai K, Handa JT. CTGF is increased in Basal Deposits and Regulates Matrix Production through the ERK (p42/p44mapk) MAPK and the p38 mapk signaling pathways. Invest Ophthalmol Vis Sci 2008;50:1903–10. [PubMed: 19011018]

Ogueta SB, Schwartz SD, Yamashita CK, Farber DB. Estrogen Receptor in the Human Eye: Influence of Gender and Age on Gene Expression. Invest Ophthalmol Vis Sci 1999;40:1906–11. [PubMed: 10440242]

Prins GS, Korach KS. The role of estrogens and estrogen receptors in normal prostate growth and disease. Steroids 2008;73:233–44. [PubMed: 18093629]

Saville B, Wormke M, Wang F, Nguyen T, Enmark E, Kuiper G, Gustafsson JA, Safe S. Ligand-, cell-, and estrogen receptor subtype (alpha/beta)-dependent activation at GC-rich (Sp1) promoter elements. J Biol Chem 2000;275:5379–87. [PubMed: 10681512]

Tusher VG, Tibshirani R, Chu G. Significance analysis of microarrays applied to the ionizing radiation response. Proc Natl Acad Sci U S A 2001;98:5116–21. [PubMed: 11309499]

Wingrove CS, Garr E, Godsland IF, Stevenson JC. 17beta-oestradiol enhances release of matrix metalloproteinase-2 from human vascular smooth muscle cells. Biochim Biophys Acta 1998;1406:169–74. [PubMed: 9573355]

Zhang D, Brodt P. Type 1 insulin-like growth factor regulates MT1-MMP synthesis and tumor invasion via PI 3-kinase/Akt signaling. Oncogene 2003;22:974–82. [PubMed: 12592384]

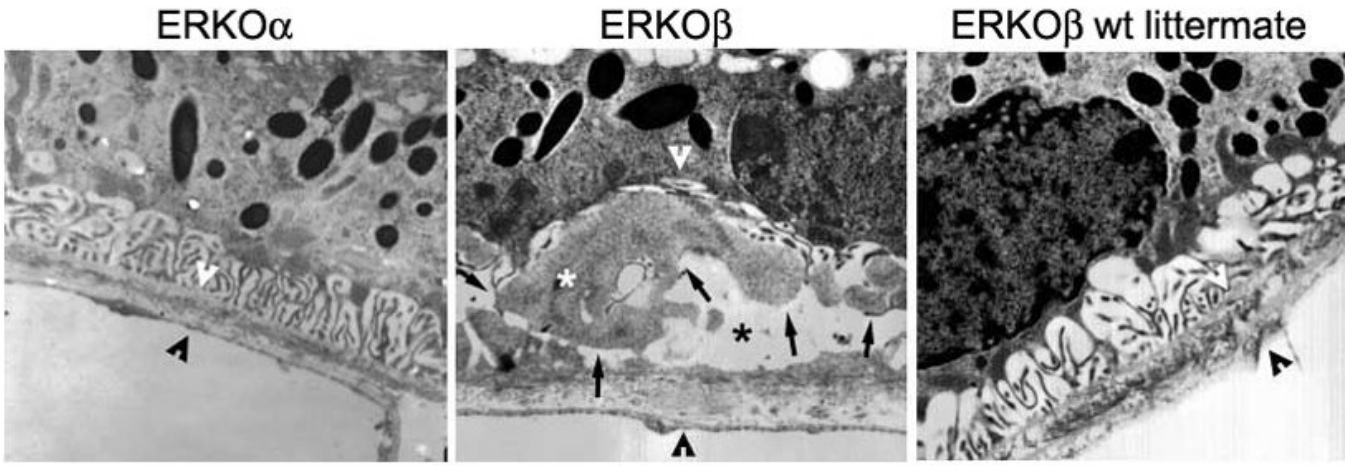

Figure 1. Ultrastructure comparison of subRPE deposits in ERKO*α*, ERKOβ and littermate control female mice fed a high fat diet and exposed to blue light

(A) Outer retina and choroid of an ERKOα mouse showed a normal RPE, BrM, and choriocapillaris with preserved basal membranous infolds (**B**) ERKOβ mouse outer retina and choroid of a mouse revealed sub-RPE deposits characterized by accumulation of moderately severe BLD with dense granular material between the RPE and its basement membrane (**black arrows**), compatible with a high mean severity score (5.75 ± 2.1). These subRPE deposits contained banded structures consistent with basal laminar deposits (**white** *) and **caused extensive destruction of membranous infolds** (**black** *). BrM was thickened (please see space between arrowheads; compared to space delineated in A and C) and the choriocapillaris was probably normal. (**C**) Outer retina and choroid of an ERKOβ wt littermate mouse also showed a normal RPE, BrM, and choriocapillaris very similar to the ERKOα mouse (please refer to the severity score table 1). Magnification: (**A** through **C**) ×25,000.

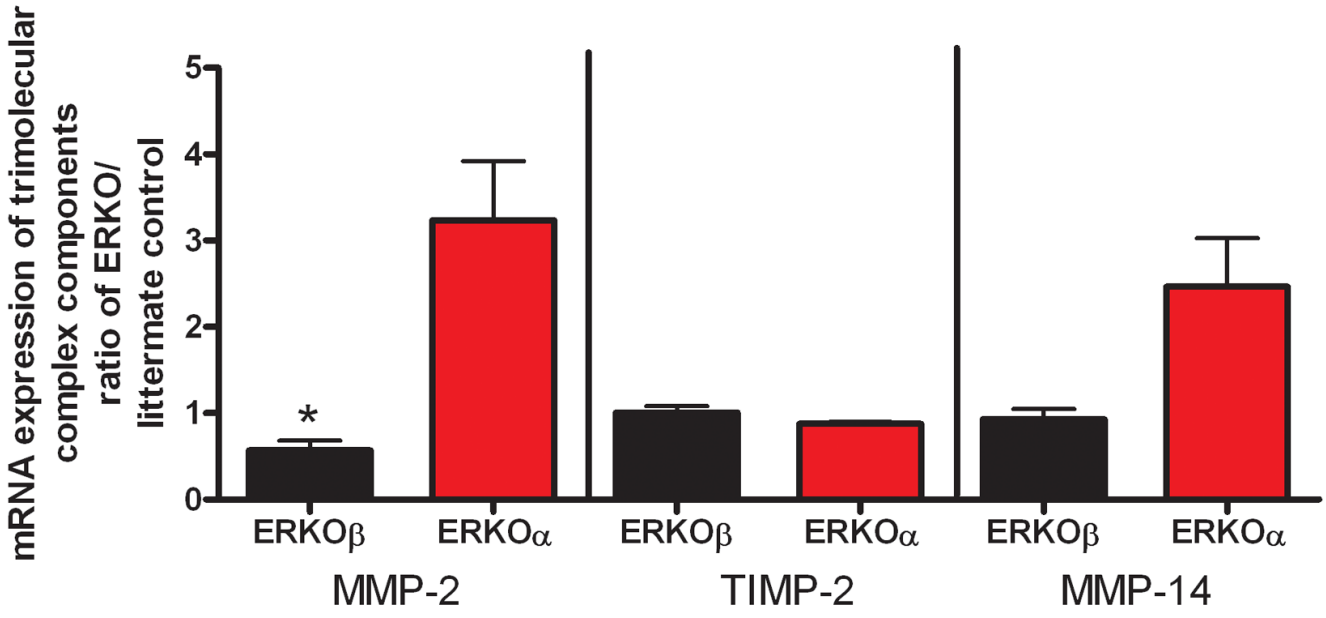

Figure 2. Components of the trimolecular complex are altered in RPE cells isolated from ERKOβ mice

mRNA expression was measured as described in methods. Data are mean of 3 experiments and calculated as fold difference from littermate ERKOβ controls for ERKOβ mice and fold difference from littermate ERKOα controls for ERKOα mice. MMP-2 mRNA expression * $p<0.05$ compared to ERKOα. All values were calculated based on ratios of target molecule/ 18s.

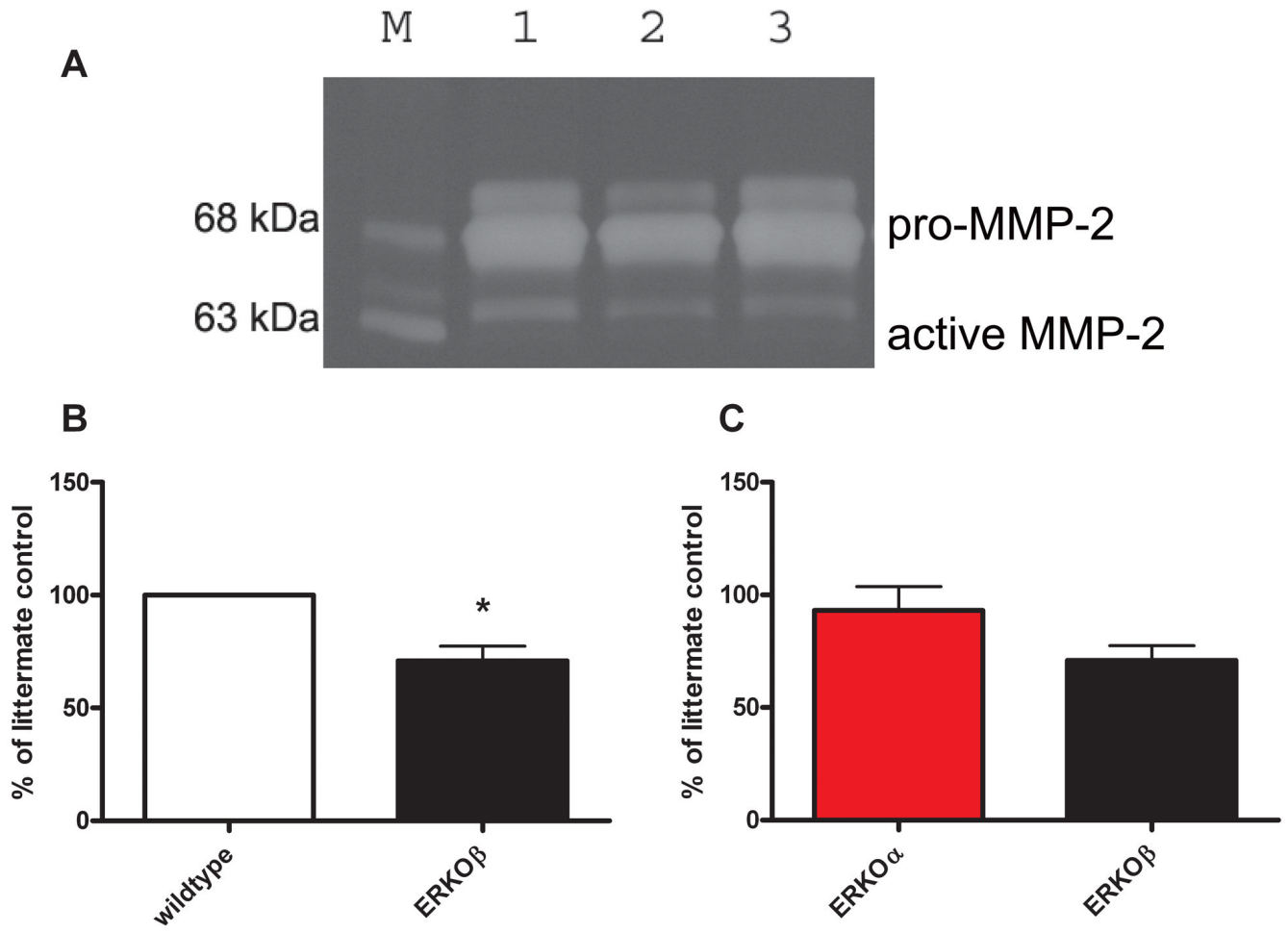

Figure 3. RPE cells isolated from ERKOβ mice have decreased pro and active MMP-2 compared to either littermate controls (B) or ERKOα (C)

(A) Representative zymogragm of cell supernatants collected from RPE cells isolated from littermate controls (wt, lane 1), ERKOβ (lane 2) or ERKOα (lane 3) mice exposed to *in vivo* oxidant injury, as detailed in the methods section. Three bands are present in the zymography; the largest band is the pro band, the lower band is the active band, and the band above the pro band is the slightly glycosylated form unique to murine cells and tissues. Data are graphed as the mean ± SEM of the active band (lower band, 63kDa). N=3 individual experiments. *p<0.05

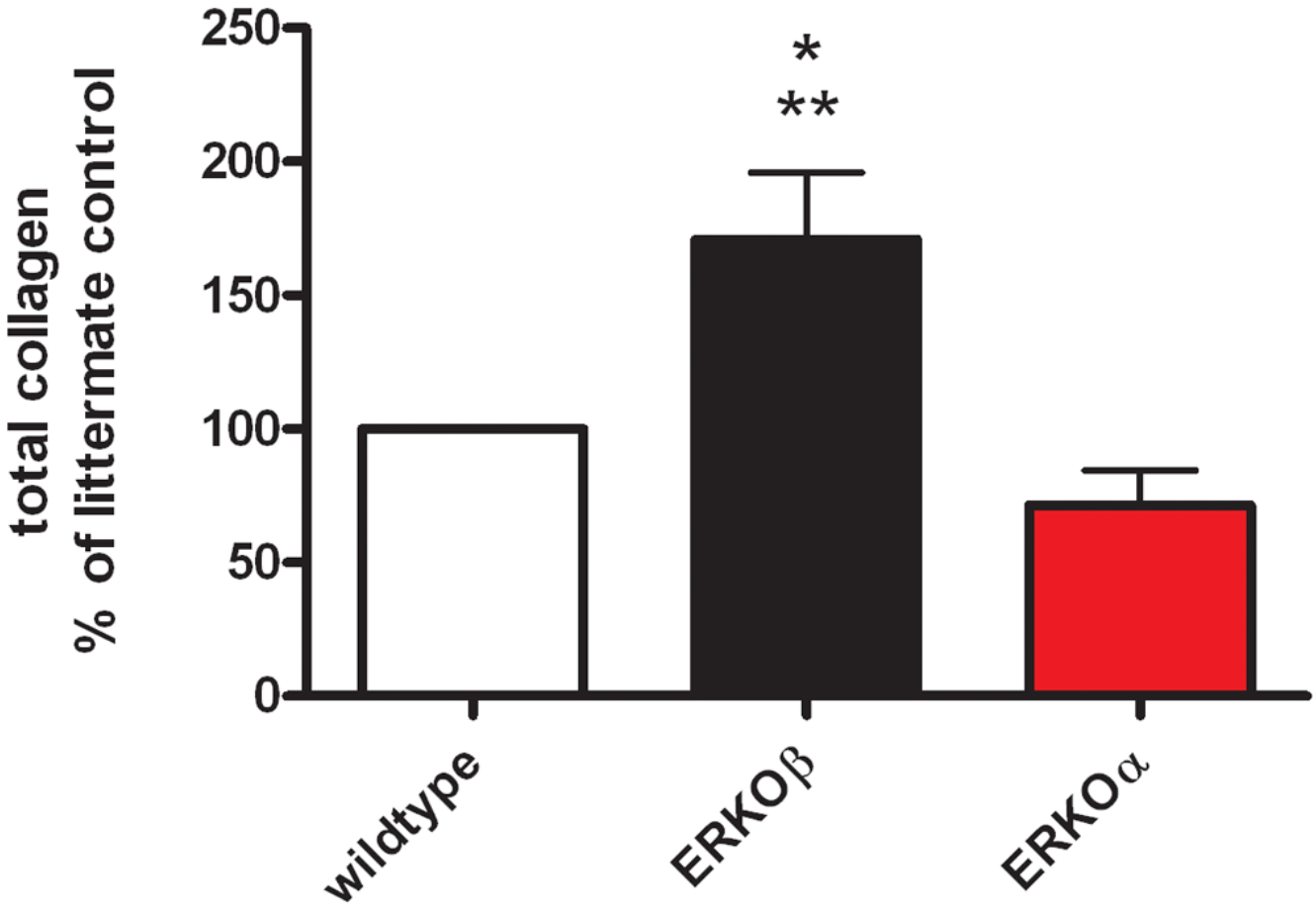

Figure 4. Collagen production of RPE cells isolated from ERKOβ mice is increased

Cell supernatants were assayed for total collagen production as described in methods. N=3 * $p<0.05$ compared to littermate control cells, ** $p<0.005$ compared to ERKOα cells.

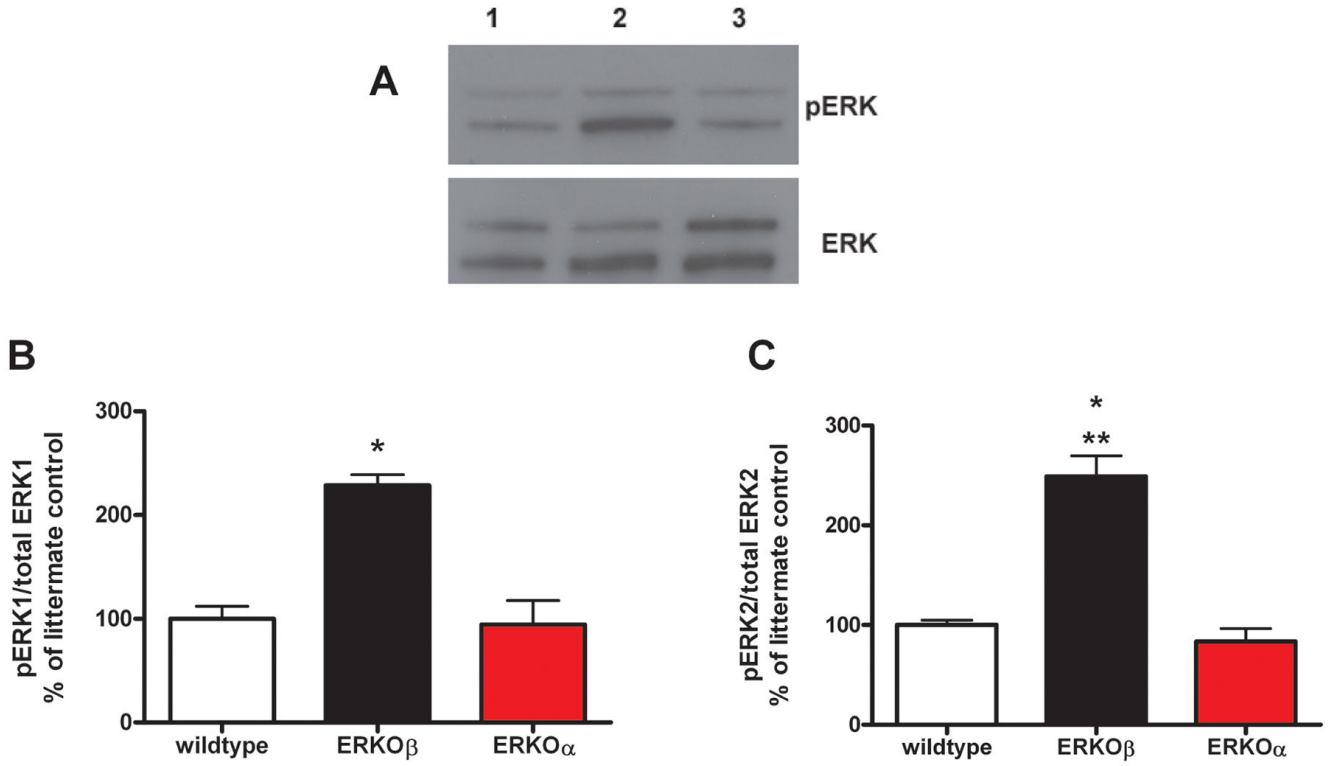

Figure 5. ERβ knockout induces ERK activation

Cell lysates were collected in duplicate from littermate controls (lane 1), ERKOβ (lane 2) and ERKOα (lane 3) RPE cell lines as described in methods. A. Representative western blots of pERK and total ERK. Data are graphed as % of littermate control cell pERK/ERK expression. B. ratio of pERK1/ERK, C. ratio of pERK2/ERK expression. N= 2 experiments using duplicate wells/treatment. * $p<0.05$ compared to littermate control (graph B and C) and ERKOα cells (graph B), ** $p < 0.005$ compared to ERKO (graph C).

Table 1

Table 1A. Effect of high fat diet, and blue light on deposit severity in ERKOα mice and littermate controls		
Mouse type	**Number of animals**	**Mean Severity Score**
ERKOα	4	2.1 ± 2.1
Littermate ERKOα	3	2.9 ± 2.9
Table 1B. Effect of high fat diet, and blue light on deposit severity in ERKOβ mice and littermate controls		
Mouse type	**Number of animals**	**Mean Severity Score**
ERKOβ	4	5.75 ± 2.1*
Littermate ERKOβ	3	2.1 ± 1.08

* p <0.05, ERKOβ vs littermate ERKOβ controls

ERKOβ vs ERKOα p=0.5

Five parameters were used for scoring the micrographs as described in methods;

1. Continuity of basal laminar deposits (BLD)
2. Maximal thickness of BLD
3. Nature of deposit content (homogeneous, banded structures, membranous debris, granular material)
4. Presence of Bruch's membrane abnormalities (including thickness analysis) and
5. Assessment of other choriocapillaris endothelial damage or invasion.